Gain Margin and Phase Margin Analysis of a Nuclear Reactor Control System with Multiple Transport Lags

C. H. CHANG AND K. W. HAN

Abstract—**A method for finding the boundaries of constant gain margin and phase margin of control systems with transport lags and adjustable parameters is presented. The considered systems are first modified by adding a gain-phase margin tester, then the characteristic equations are formulated, and finally the stability equations are used to find the boundaries of constant gain margin and phase margin. The main advantage of the proposed method is to obtain complete information about the effects of adjustable parameters on gain margin and phase margin and their corresponding crossover frequencies. In order to show the usefulness of the proposed method a nuclear reactor control system with multiple transport lags is chosen as one of the examples.**

I. Introduction

FOR THE ANALYSIS and design of practical control systems, gain margin (GM) and phase margin are the two important specifications. The frequency domain approach, based upon the works of Nyquist, Bode, and Nichols, permits a designer to find these two values in a sample manner [1]. However, this approach is unsuitable for systems with two or more adjustable parameters.

Control system containing transport lags are usually difficult to analyze due to the existance of exponential functions in system transfer functions. Lawrence Eisenberg has analyzed a system with a transport lag using the parameter plane method [2]. Hu and Han have presented a method to analyze control systems with multiple transport lags and multiple adjustable parameters using the parameter plane and parameter space methods [3]. However, all these methods cannot give information on gain margin and phase margin.

The main purpose of this paper is to present a method to find gain margin and phase margin of control systems with transport lags and adjustable parameters. Based upon the proposed method, the boundaries of constant gain margin and phase margin can be plotted in a parameter plane or a parameter space. For each selected point on these boundaries the specific phase margin and gain margin are the same as those obtained by use of a Nyquist diagram.

The proposed method is advantageous because the effects on phase margin and gain margin due to parameter variations can be clearly defined, simplifying design work by adjusting parameters to obtain desirable gain margin and phase margin and their corresponding crossover frequencies. As an illustration, the nuclear reactor control system considered by Hu and Han in [3] is reconsidered in this paper.

Manuscript received March 31, 1989; revised April 27, 1989.

C. H. Chang is with the Institute of Electronics, National Chiao-Tung University, Taiwan, Republic of China.

K. W. Han is with Chung-Shan Institute and National Chiao-Tung University, Hsinchu, Taiwan, Republic of China.

IEEE Log Number 8930161.

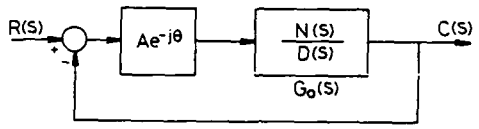

Fig. 1. Control system with a gain-phase margin tester.

II. The Basic Method

Consider the system shown in Fig. 1 where $G_0(s)$ is the open loop transfer function which may have exponential functions (e^{-sT_i}) due to transport lags (see the Nomenclature). A gain-phase margin tester represented by $Ae^{-j\Theta}$ is added to $G_0(s)$ for plotting the boundaries of constant gain margin and phase margin as explained later.

The characteristic equation of the system is

$$F(s)=1+Ae^{-j\Theta}G_0(s)=D(s)+Ae^{-j\Theta}N(s)=0. \quad (1)$$

Let $s = j\omega$, then (1) can be written as

$$F(j\omega)=F(\alpha, \beta, \gamma, \cdots, T_1, T_2, \cdots, T_i, A, \Theta, j\omega)=0 \quad (2)$$

where $\alpha, \beta, \gamma, \cdots$ are variable and/or adjustable parameters, and $T_1, T_2, \cdots, T_i$ are constants due to transport lags. Decomposing the characteristic equation into two stability equations, i.e., the real part (Fr) and the imaginary part (Fi) of $F(j\omega)$, one has

$$Fr(\alpha, \beta, \gamma, \cdots, T_1, T_2, \cdots, T_i, A, \Theta, \omega)=0 \quad (3)$$

and

$$Fi(\alpha, \beta, \gamma, \cdots, T_1, T_2, \cdots, T_i, A, \Theta, \omega)=0. \quad (4)$$

Assume that (3) and (4) are linear functions of α and β, then one has

$$Fr(\alpha, \beta, \gamma, \cdots, T_1, T_2, \cdots, T_i, A, \Theta, \omega) = \alpha \cdot B_1+\beta \cdot C_1+D_1=0 \quad (5)$$

$$Fi(\alpha, \beta, \gamma, \cdots, T_1, T_2, \cdots, T_i, A, \Theta, \omega) = \alpha \cdot B_2+\beta \cdot C_2+D_2=0 \quad (6)$$

0018-9499/89/0800-1418$01.00

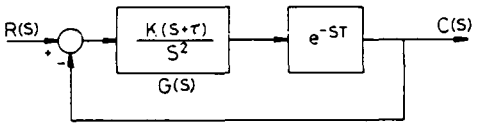

Fig. 2. Block diagram of control system with transport lag.

where B_1, B_2, C_1, C_2, D_1, and D_2 are functions of $\gamma \cdots$, T_1, T_2, $\cdots$, T_i, A, Θ, and ω. Solving (5) and (6) for α and β, one has [4], [5]

$$\alpha = \frac{C_1 \cdot D_2 - C_2 \cdot D_1}{\Delta} \tag{7}$$

$$\beta = \frac{D_1 \cdot B_2 - D_2 \cdot B_1}{\Delta} \tag{8}$$

where

$$\Delta = B_1 \cdot C_2 - B_2 \cdot C_1. \tag{9}$$

If (5) and (6) are not linear functions of α and β, theoretically α and β can be solved also since there are two independent equations [5].

In (7) and (8), let $A = 0$ dB (i.e., $A = 1$) and $\Theta = 0$, and set $\gamma, \cdots, T_1, T_2, \cdots, T_i$ equal to constants, then for various values of ω, a locus that contains the stability boundary of the system can be plotted in the α versus β plane. Each point on this locus represents a condition of the system to have its Nyquist plot of $G_0(s)$ passing through the critical point $(-1, j0)$, i.e., to have a pair of characteristic roots on the imaginary axis of the s-plane. If A is assumed equal to a constant and $\Theta = 0$, the locus in the α versus β plane is a boundary of constant gain margin. On the other hand, if $A = 0$dB, and Θ is assumed equal to a constant, the locus is a boundary of constant phase margin. The corresponding values of ω on the constant gain-margin boundary and the constant phase-margin boundary are the phase crossover frequency and the gain crossover frequency, respectively. For several values of γ a subspace can be found in the three dimensional parameter space using γ as the third axis [6]–[8].

In general, the stability boundary is plotted first, and then the boundaries of constant gain margin and phase margin are plotted in the stable region. The rule for finding the stable region for the stability boundary is that, facing the direction in which ω is increasing, if Δ defined in (9) is positive (negative), the left (right) side of the stability boundary is the stable region.

III. Examples

The main purposes of this section are to reconsider the examples analyzed in [2] and [3] and to obtain complete information on boundaries of constant gain margin and phase margin.

Example 1 [2]: Consider the system shown in Fig. 2. The open loop transfer function is

$$G_0(s) = \frac{K(s+\tau)e^{-sT}}{s^2}. \tag{10}$$

Defining $\alpha = K$, $\beta = K\tau$, setting $s = j\omega$, and adding the gain-phase margin tester to the system, the characteristic equation is

$$\begin{aligned} F(j\omega) &= 1 + Ae^{-j\Theta}G_0(j\omega) \\ &= -\omega^2 + A(\cos\Theta - j\sin\Theta)(j\alpha\omega + \beta) \\ &\quad \cdot (\cos\omega T - j\sin\omega T) = 0. \end{aligned} \tag{11}$$

After some algebraic manipulations, the two stability equations can be expressed as

$$\begin{aligned} Fr(\alpha, \beta, T, A, \Theta, \omega) &= \alpha \cdot B_1 + \beta \cdot C_1 + D_1 \\ &= \alpha \cdot [A\omega \sin(\omega T + \Theta)] \\ &\quad + \beta[A\cos(\omega T + \Theta)] + [-\omega_2] \end{aligned} \tag{12}$$

$$\begin{aligned} Fi(\alpha, \beta, T, A, \Theta, \omega) &= \alpha \cdot B_2 + \beta \cdot C_2 + D_2 \\ &= \alpha \cdot [A\omega \cos(\omega T + \Theta)] \\ &\quad + \beta \cdot [-A\sin(\omega T + \Theta)] + [0]. \end{aligned} \tag{13}$$

Assuming $T = 1$, using (7) to (9), and letting ω vary from zero to infinity, the stability boundary (by setting $A = 0$ dB and $\Theta = 0$), the constant gain-margin boundary (by setting $A = 6$ dB and $\Theta = 0$), and the constant phase-margin boundary (by setting $A = 0$ dB and $\theta = 30°$) are plotted in the α vs. β plane as shown in Fig. 3. It can be seen that these three boundaries divide this parameter plane into several regions, where the region denoted by R_1 is the stable region [2]. For better understanding of R_1 an enlarged figure is shown in Fig. 4, where each region has its specific gain margin and phase margin (PM). For example, the region denoted by R_{11} represents GM $>$ 6 dB, and PM $>$ 30°. Similarly, R_{12} represents GM $>$ 6 dB and 30° $>$ PM $>$ 0°. If α and β are adjusted to point $P_0(\alpha = 0.686, \beta = 0.166)$, the gain margin and phase margin will be 6 db and 30°, respectively. The corresponding phase crossover frequency (ω_{cp}) and gain crossover frequency (ω_{cg}) are at 1.396 rad/s and 0.724 rad/s, respectively. Therefore, a designer can select desirable values of parameters to make the system meet specifications on gain

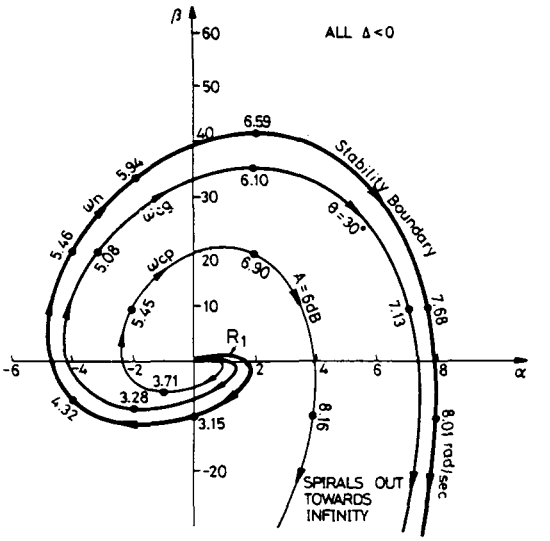

Fig. 3. Boundaries of stability constant gain margin and constant phase margin in α versus β plane.

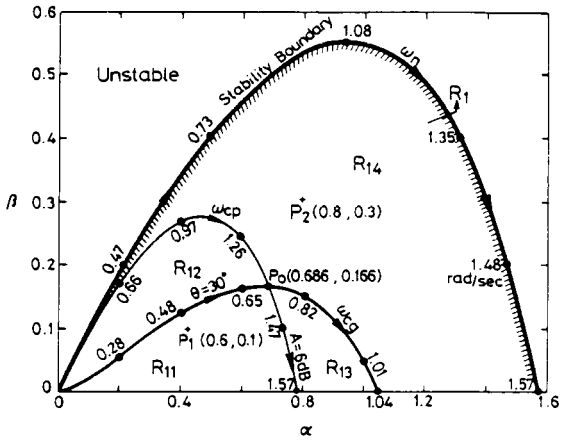

Fig. 4. Enlarged boundaries of Fig. 3.

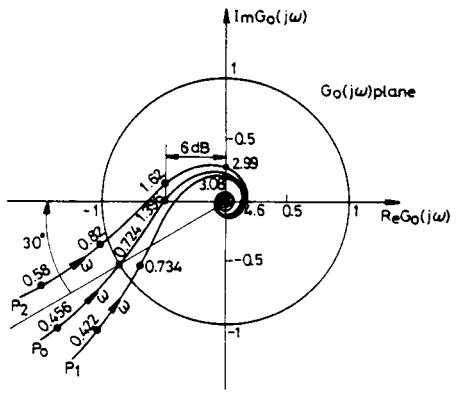

Fig. 5. Nyquist plots of Example 1.

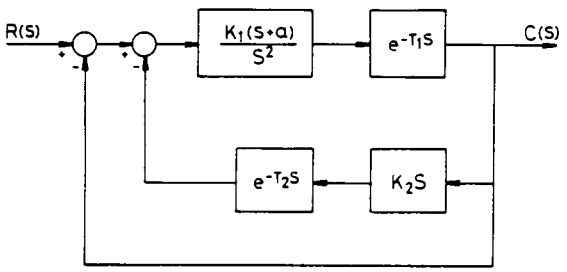

Fig. 6. Block diagram of control system with two transport lags.

margin and phase margin simply by looking at the few boundaries shown in Fig. 4.

In order to check the results in Fig. 4, three points $P_0(\alpha = 0.686, \beta = 0.166)$, $P_1(\alpha = 0.6, \beta = 0.1)$ and $P_2(\alpha = 0.8, \beta = 0.3)$ are selected, and the corresponding Nyquist plots are shown in Fig. 5. From Figs. 4 and 5 it can be seen that, for analysis and design of a system with multiple adjustable parameters, to plot the boundaries of constant gain margin and phase margin is better than plotting several Nyquist plots.

Example 2 [3]: A control system with two transport lags and multiple adjustable parameters is shown in Fig. 6, where a, K_1, and K_2 are adjustable parameters; T_1 and T_2 are transport lags. Assume that the purpose of analysis and design is to find the ranges of parameters such that the system is stable and has phase margin and gain margin defined as $60° >$ PM $> 30°$ and GM > 6 dB, respectively.

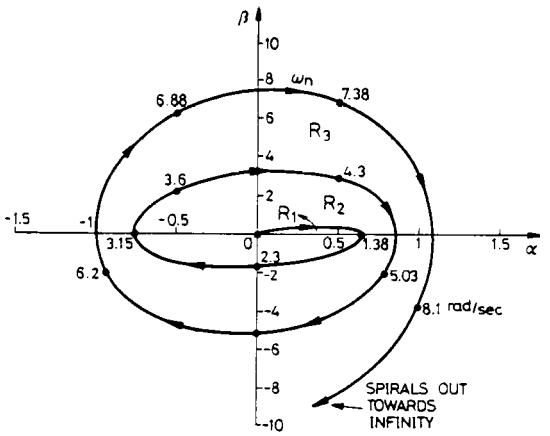

Fig. 7. Stability boundary of Example 2.

The open loop transfer function of the system is

$$G_0(s) = \frac{K_1(s+a)e^{-T_1 s}}{s^2 + K_1K_2s(s+a)e^{-(T_1+T_2)s}}. \tag{14}$$

After adding a gain-phase margin tester, the characteristic equation is

$$F(s) = s^2 + K_1K_2s(s+a)e^{-(T_1+T_2)s} + Ae^{-j\Theta}K_1(s+a)e^{-T_1 s} = 0. \tag{15}$$

Defining $K_1 = \alpha$, $K_1 a = \beta$, $K_2 = \gamma$, and setting $s = j\omega$, the stability equations are found as

$$\begin{aligned} Fr(\alpha, \beta, \gamma, T_1, T_2, A, \Theta, \omega) &= \alpha \cdot B_1 + \beta \cdot C_1 + D_1 \\ &= \alpha \cdot [-\gamma\omega^2 \cos(T_1\omega + T_2\omega) + A\omega \sin(T_1\omega + \Theta)] \\ &\quad + \beta \cdot [\gamma\omega \sin(T_1\omega + T_2\omega) + A \cos(T_1\omega + \Theta)] + [-\omega^2] \end{aligned} \tag{16}$$

$$\begin{aligned} Fi(\alpha, \beta, \gamma, T_1, T_2, A, \Theta, \omega) &= \alpha \cdot B_2 + \beta \cdot C_2 + D_2 \\ &= \alpha \cdot [\gamma\omega^2 \sin(T_1\omega + T_2\omega) + A\omega \cos(T_1\omega + \Theta)] \\ &\quad + \beta \cdot [\gamma\omega \cos(T_1\omega + T_2\omega) - A \sin(T_1\omega + \Theta)] + [0]. \end{aligned} \tag{17}$$

Assuming $T_1 = 1.5$, $T_2 = 0.5$, and $\gamma = 1$, and using of the same approach as in Example 1, the stability boundary is plotted as shown in Fig. 7, where R_1 is the stable region [3]. The details of R_1 are shown in Fig. 8, which indicates that the boundaries of constant gain margin ($A = 6$ dB) and constant phase margins ($\Theta = 30°$ and $\Theta = 60°$) divide the stable region R_1 into six regions, and that the region marked by R_{11} is the desirable one for having GM > 6 dB and $60° >$ PM $> 30°$.

In order to find the effect of the third parameter γ, several values are assigned to it, and the corresponding boundaries in parameter plane are found. Then a subspace with GM > 6db and $60° >$ PM $> 30°$ in a three dimensional parameter space

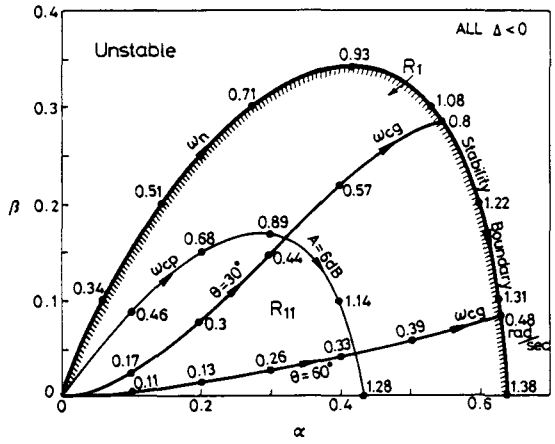

Fig. 8. Boundaries of constant gain margin and phase margins in stable region.

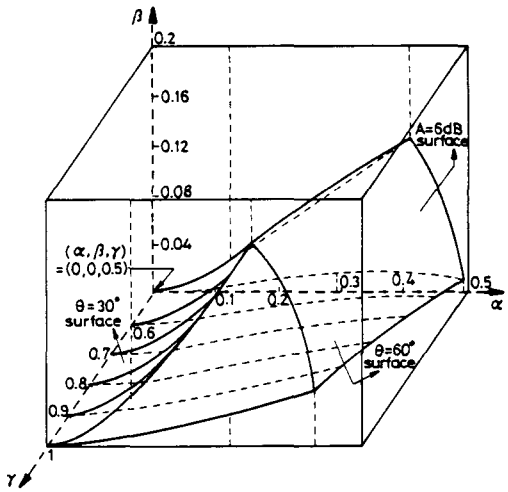

Fig. 9. A subspace for GM > 6 dB and 60° > PM > 30°.

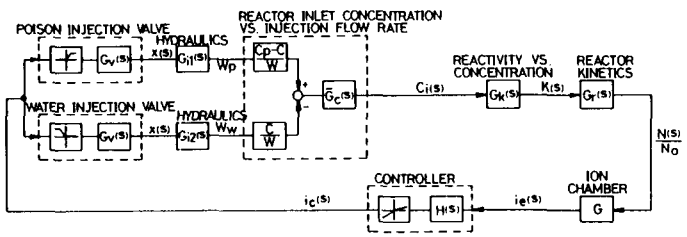

Fig. 10. Block diagram of reactor control system.

can be constructed as shown in Fig. 9. Inside this subspace any point selected will represent a set of values of α, β, and γ to make the system stable and meet specifications (60° > PM > 30° and GM > 6 dB). The results in this example have been checked by use of Nyquist plots also.

Example 3: A chemical system operated for the automatic fine control of a nuclear reactor is considered in this example, [1], [3]. The system block diagram is given in Fig. 10. For simplicity, the system is considered linear, and the transfer functions of the blocks are as follows.

1) Injection valves

$$G_v = \frac{x(s)}{i_c(s)} = \frac{G_v(0)}{(s/\omega_0)^2 + 2\zeta(s/\omega_0) + 1}. \tag{18}$$

2) Flow rate versus injection valve opening

$$G_{i1} = \frac{W_i(s)}{x(s)} = \frac{1}{C_v}\left(\frac{P_0 - P_b}{g\rho}\right)^{1/2} = \text{constant} \tag{19}$$

$$G_{i2} = \frac{W(s)}{x(s)} = \frac{1}{C_v}\left(\frac{P_0 - P_b}{g\rho}\right)^{1/2} \frac{\alpha_e s + 2X_e W - dH/dW}{\alpha' s + 2XW - dH/dW} \tag{20}$$

where C_v is a constant, and the time constants may be neglected in comparison with others affecting the system dynamics [1].

3) Poison concentration versus injection flow rate

$$G_c(s) = \frac{C_i(s)}{W_i(s)} = a\bar{G}_c(s) = a\,\frac{\exp(-sT_1)/(1+s\tau_1)}{1 - \exp(-sT)/(1+s\tau_1)(1+s\tau_2)} \tag{21}$$

where $a = (C_p - C)/W$ or C/W for poison or water injection respectively.

4) Reactivity versus concentration

$$G_k(s) = \frac{K'(s)}{C_i(s)} = \left(\frac{dK}{dC}\right)_c \frac{1 - \exp(-sT_r)}{T_r s[1 + (sT_r/4\pi)^2]} \tag{22}$$

where $(dK/dC)_c$ is the slope of the characteristic given the reactivity versus poison concentration at steady state [1].

5) Nuclear power versus reactivity

$$G_r(s) = \frac{N(s)}{N_o K(s)} = 1/N_o s(l^* + \Sigma_i \beta_i/s + \lambda_i). \tag{23}$$

The ion chamber transfer function is assumed to be a constant gain (G).

The open loop system transfer function is

$$G_o(s) = \frac{G_o T^* \exp(-sT_1)/(1+s\tau_1)}{1 - \exp(-sT)/(1+s\tau_1)(1+s\tau_2)} \times \frac{1 - \exp(-sT_r)}{sT_r[1 + (sT_r/4\pi)^2]} \times \frac{1}{(s/\omega_0)^2 + 2\zeta(s/\omega_0) + 1} \times G_r(s) \tag{24}$$

where G_o is the open loop gain. After simplification (24) becomes

$$G_o(s) = \frac{K(s + 1/\tau_2)e^{-sT_1}(1 - e^{-sT_r})}{s^2(s^2 + 16\pi/T_r^2)(s^2 + 2\zeta\omega_0 s + \omega_0^2)} \times \frac{G_r'(s)}{[(s + 1/\tau_1)(s + 1/\tau_2) - e^{-sT}/\tau_1\tau_2]} \tag{25}$$

where

$$K = (16\pi^2\omega_0^2 T^* G_0)/\tau_1 T_r^3 N_o \tag{26}$$

$$G_r'(s) = 1/(l^* + \Sigma_i \beta_i/s + \lambda_i). \tag{27}$$

Note that one pole of $G_r(s)$ in (23) is combined with the pole of (25), and the steady state reactor power (N_o) is included in K. Thus the parametric investigation of the reactor power as

well as the open loop gain can be investigated by changing the parameter K.

In this case, the following values are given as constants, such as: $T_1 = 4$ s; $T_r = 0.6$ s; $\tau_1 = 0.25$ s; $\tau_2 = 1.3$ s; $\omega_0 = 5$ s; $\zeta = 0.8$; and the values of $\beta_i$and λ_i are stated by Keepin [9], then $G_r'(s)$ can be rewritten as

$$G_r'(s) = 1/(l^* + \Sigma_i \beta_i/s + \lambda_i) = \frac{\Pi_i(s+\lambda_i)}{l^*\Pi_i(s+\lambda_i) + \Sigma_i \beta_i \Pi_{j\neq i}(s+\lambda_j)}$$

$$= \frac{G_\lambda(s)}{l^* G_\lambda(s) + G_\beta(s)} \tag{28}$$

where

$$G_\lambda(s) = \Pi_i(s+\lambda_i)$$
$$= s^6 + 4.5549s^5 + 5.216554s^4 + 1.71376s^3 + 0.176s^2 + 0.0053s + 0.0000417 \tag{29}$$

$$G_\beta(s) = \Sigma_i \beta_i \Pi_{j\neq i}(s+\lambda_j)$$
$$= 0.00645s^5 + 0.0268s^4 + 0.0255s^3 + 0.00554s^2 + 0.000318s + 0.00000349. \tag{30}$$

From (25), the open loop transfer function becomes

$$G_o(s) = \frac{K(s+0.7692307)e^{-4s}}{s^2(s^2+438.6483)(s^2+8s+25)} \times \frac{(1-e^{-0.6s})}{s^2+4.76923s+3.076923-3.076923e^{-Ts}} \times \frac{G_{\lambda(s)}}{l^* G_\lambda(s) + G_\beta(s)}. \tag{31}$$

After adding a gain-phase margin tester the characteristic equation is

$$F(s) = 1 + Ae^{-j\Theta}G_o(s)$$
$$= s^2(s^2+438.6483)(s^2+8s+25)(s^2+4.76923s + 3.076923 - 3.076923e^{-Ts}) \times [l^* G_\lambda(s) + G_\beta(s)] + Ae^{-j\Theta}K(s+0.7692307) \cdot e^{-4s}(1-e^{-0.6s})G_\lambda(s) = 0. \tag{32}$$

Letting K and l^* be two parameters and setting $s = j\omega$, after some algebraic manipulations, the two stability equations can be expressed with the same forms as (5) and (6); they are

$$Fr(K, l^*, T, A, \Theta, \omega) = K \cdot B_1 + l^* \cdot C_1 + D_1 \tag{33}$$

$$Fi(K, l^*, T, A, \Theta, \omega) = K \cdot B_2 + l^* \cdot C_2 + D_2 \tag{34}$$

where

$$B_1 = A\{(-a_6\omega^6 + a_4\omega^4 - a_2\omega^2 + a_0) \cdot [\cos(4\omega+\Theta) - \cos(4.6\omega+\Theta)] + (-a_7\omega^7 + a_5\omega^5 - a_3\omega^3 + a_1\omega) \cdot [\sin(4\omega+\Theta) - \sin(4.6\omega+\Theta)]\} \tag{35}$$

$$C_1 = (-b_{14}\omega^{14} + b_{12}\omega^{12} - b_{10}\omega^{10} + b_8\omega^8 - b_6\omega^6 + b_4\omega^4 - b_2\omega^2) - (c_{12}\omega^{12} - c_{10}\omega^{10} + c_8\omega^8 - c_6\omega^6 + c_4\omega^4 - c_2\omega^2)[\cos(T\omega)] - (-c_{11}\omega^{11} + c_9\omega^9 - c_7\omega^7 + c_5\omega^5 - c_3\omega^3)[\sin(T\omega)] \tag{36}$$

$$D_1 = (d_{12}\omega^{12} - d_{10}\omega^{10} + d_8\omega^8 - d_6\omega^6 + d_4\omega^4 - d_2\omega^2) - (-e_{10}\omega^{10} + e_8\omega^8 - e_6\omega^6 + e_4\omega^4 - e_2\omega^2)[\cos(T\omega)] - (-e_{11}\omega^{11} + e_9\omega^9 - e_7\omega^7 + e_5\omega^5 - e_3\omega^3)[\sin(T\omega)] \tag{37}$$

$$B_2 = A\{(-a_7\omega^7 + a_5\omega^5 - a_3\omega^3 + a_1\omega) \cdot [\cos(4\omega+\Theta) - \cos(4.6\omega+\Theta)] - (-a_6\omega^6 + a_4\omega^4 - a_2\omega^2 + a_0) \cdot [\sin(4\omega+\Theta) - \sin(4.6\omega+\Theta)]\} \tag{38}$$

$$C_2 = (b_{13}\omega^{13} - b_{11}\omega^{11} + b_9\omega^9 - b_7\omega^7 + b_5\omega^5 - b_3\omega^3) - (-c_{11}\omega^{11} + c_9\omega^9 - c_7\omega^7 + c_5\omega^5 - c_3\omega^3)[\cos(T\omega)] + (c_{12}\omega^{12} - c_{10}\omega^{10} + c_8\omega^8 - c_6\omega^6 + c_4\omega^4 - c_2\omega^2)[\sin(T\omega)] \tag{39}$$

$$D_2 = (d_{13}\omega^{13} - d_{11}\omega^{11} + d_9\omega^9 - d_7\omega^7 + d_5\omega^5 - d_3\omega^3) - (-e_{11}\omega^{11} + e_9\omega^9 - e_7\omega^7 + e_5\omega^5 - e_3\omega^3)[\cos(T\omega)] + (-e_{10}\omega^{10} + e_8\omega^8 - e_6\omega^6 + e_4\omega^4 - e_2\omega^2)[\sin(T\omega)] \tag{40}$$

where the values of $a's$, $b's$, $c's$ and $d's$ are tabulated in the Appendix.

Setting $T = 9.3$, and applying the same approach as before, the stability boundary, the boundary of constant gain margin ($A = 6$db) and the boundaries of constant phase margins ($\Theta = 30°$, $\Theta = 37.2°$) can be plotted in a K versus l^* plane as shown in Fig. 11, which indicates that the region denoted by R_0 is the region for $A > 6$ dB and $\Theta > 30°$. For example, if K and l^* are adjusted to point $P_2(K = 247, l^* = 0.0272)$, the system will have a gain margin at $A = 6$ dB and a phase margin at $\Theta = 30°$. The corresponding phase crossover frequency (ω_{cp}) and gain crossover frequency (ω_{cg}) are at 0.555 rad/s and 0.075 rad/s, respectively. It can be seen that if the gain margin is limited at 6 dB, the maximum phase margin is approximately at 37.2°, because the boundary for $\Theta = 37.2°$ is tangent to the boundary for $A = 6$db at point P_1.

If point $P_0(K = 100, l^* = 0.02)$ in the region R_0 is selected, its Nyquist plot is shown in Fig. 12, and its Bode diagram is shown in Fig. 13. From these two figures one obtains GM = 10.2 *dB*, *PM* = 31.2°, $\omega_{cp} = 0.563$ rad/s and

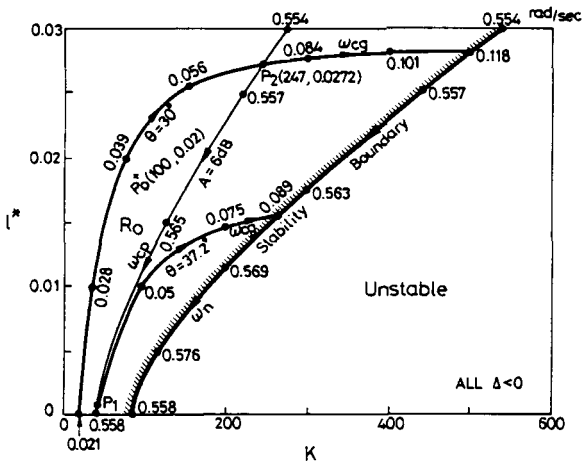

Fig. 11. The boundaries of constant gain margin and phase margins for Example 3.

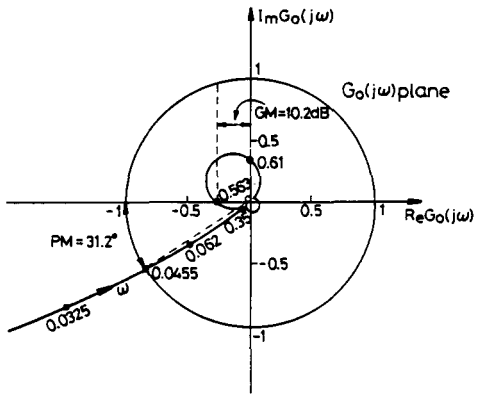

Fig. 12. The Nyquist plot for $P_0(100,0.02)$ in Fig. 11.

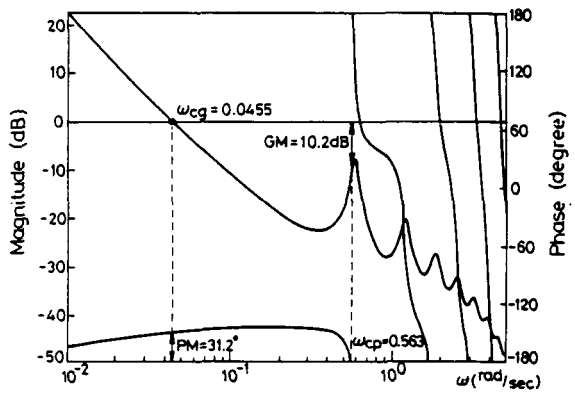

Fig. 13. The Bode diagram for $P_0(100,0.02)$ in Fig. 11.

$\omega_{cg} = 0.0455$ rad/s. Note that all these results can be predicted from Fig. 11, approximately.

In this example, although adjusting two parameters K and l^* can make the system stable and have a gain margin larger than 6 dB and phase margin larger than 30°, unfortunately the transient behavior of the system is too slow, because the maximum gain crossover frequency is 0.075 rad/s for gain margin and phase margin limited at 6 dB and 30°, respectively. In order to improve the transient response a compensator $H(s)$ is introduced [1] i.e.,

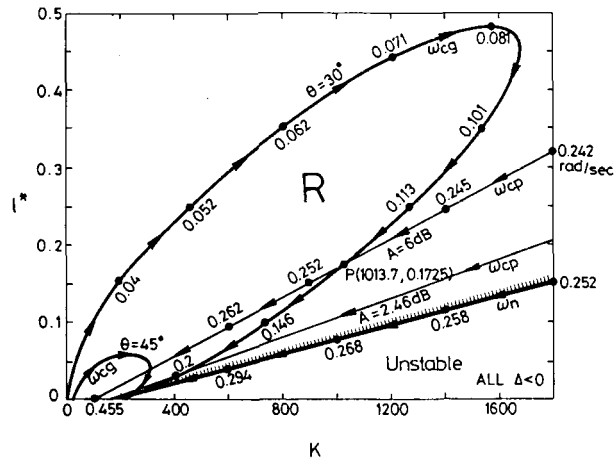

Fig. 14. The boundaries of constant gain margins and phase margins for compensated system.

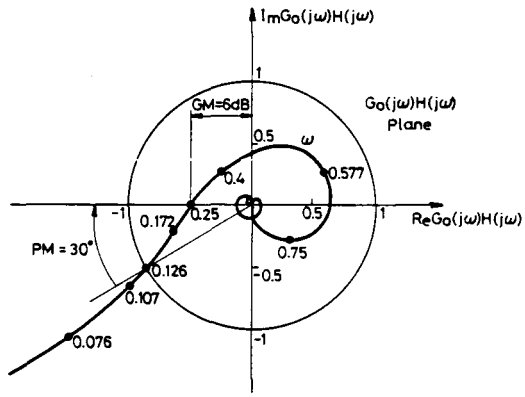

Fig. 15. The Nyquist plot for $P(1013.7, 0.1725)$ in Fig. 14.

$$H(s) = \frac{1 - e^{-sT}}{sT} \times \frac{a(s + 1/a\tau)}{s + 1/\tau} \tag{41}$$

where the first term is based upon the inverse function criterion to compensate the first term given in (24) concerning the closed loop circulation time; the second term is the lead term by $a > 1$ to compensate for the delay relative to the injection point-core inlet transit time.

Assuming $1/\tau = 0.6$ and $a = 10$, after adding $H(s)$ into the system and applying the same approach as before, the result in the K versus l^* plane is shown in Fig. 14, which indicates that the region denoted by R gives GM > 6 dB and 45° > PM > 30°. If K and l^* are adjusted to point $P(K = 1013.7, l^* = 0.1725)$, the compensated system will have a gain margin at $A = 6$ dB and a phase margin at $\Theta = 30°$. The corresponding phase crossover frequency (ω_{cp}) and gain crossover frequency (ω_{cg}) are at 0.25 rad/s and 0.126 rad/s, respectively. The Nyquist plot for $P(K = 1013.7, l^* = 0.1725)$ is shown in Fig. 15.

Note that the compensator does improves the gain crossover frequency from 0.075 rad/s to 0.126 rad/s and keep the gain margin and phase margin limited at 6 dB and 30°, respectively, In addition, Fig. 14 also shows that the compensated system can give higher gain crossover frequency by adjusting

parameters, but the higher the gain crossover frequency is the smaller the gain margin will be. For example, the gain margin will decrease to 2.46 dB if phase margin and gain crossover frequency are limited at 30° and 0.2 rad/s, respectively. In short, all the effects of adjusting parameters can be realized from the boundaries of constant gain margin and phase margin.

IV. Conclusion

A method for plotting the boundaries of constant gain margin and phase margin of control systems with multiple transport lags and adjustable parameters has been presented. The main advantage of the presented method is that the relations among gain margin, phase margin, and the adjustable parameters can be completely and easily defined. Therefore, the design work by adjusting parameters to obtain desirable gain margin and phase margin and their corresponding crossover frequencies can be simplified. Since all the analyses are based upon two stability equations that are amenable to digital computer computation, the proposed method has the potential for analysis and design of very complicated systems.

Nomenclature

C	Solution concentration.
C_i	Reactor inlet solution concentration.
C_p	Saturated solution concentration.
$F(s)$	System characteristic equation.
G_o	Open loop gain.
$G_o(s)$	Open loop transfer function.
$G_c(s)$	Hydraulic transfer function.
$\bar{G}_c(s)$	Normalized $G_c(s)$ transfer function.
$G_i(s)$	Hydraulic transfer function.
$G_k(s)$	K versus C_i transfer function.
$G(s)$	Ion chamber transfer function.
$G_r(s)$	Reactor transfer function.
$G_v(s)$	Injection valves transfer function.
g	Gravity constant.
dH/dW	Pump characteristics.
$H(s)$	Controller transfer function.
i_c	Injection valves input signal.
i_e	Ion chamber current.
K'	Reactivity excess.
K	Over all open loop gain.
L	Total loop length.
L_e	Loop Length from expansion tank to injection point.
l^*	Neutron mean lift time.
N	Nuclear power.
N_o	Steady state power.
P_b	Injection point pressure.
P_0	Injection tank pressure.
s	Laplace operator.
T	Total circulation time.
T^*	$T + \tau_1 + \tau_2$.
T_1	Injection point-reactor inlet time delay.
T_r	In-pile section transit time.
x	Injection valve fractional opening.
W	In-pile flow rate.
W_i	Injection flow rate.
W_p	Poison injection flow rate.
W_w	Water injection flow rate.
A'	Pipe cross section.
α_e	$L_e/A'g$.
α'	$L/A'g$.
β_i	Delay neutrons ith group yield.
λ_i	Delay neutrons ith group decay constants.
ρ	Solution density.
τ_1	Injection point—reactor inlet mixing time constant.
τ_2	Reactor outlet—injection point mixing time constant.
ζ	Injection valve damping ratio.
X_e	Expansion tank—injection point pressure drop factor.
X	Total pressure drop factor.
ω_0	Injection valve natural frequency.
ω_n	Natural frequency.
ω_{cp}	Phase-Crossover frequency.
ω_{cg}	Gain-crossover frequency.
α, β, γ	Parameters.

Appendix

$a_7 = 1.000000000000000E0$
$a_6 = 5.324130700000000E0$
$a_5 = 8.720322915430000E0$
$a_4 = 5.726493485007800E0$
$a_3 = 1.494276804432000E0$
$a_2 = 1.406846032000000E-1$
$a_1 = 4.118622710000000E-3$
$a_0 = 3.207692019000000E-5$

$b_{14} = 1.000000000000000E0$
$b_{13} = 1.732413000000000E1$
$b_{12} = 5.682581827270000E2$
$b_{11} = 8.113045947701120E3$
$b_{10} = 5.795283829941001E4$
$b_9 = 2.266140896816154E5$
$b_8 = 4.830338474910203E5$
$b_7 = 5.337794507432882E5$
$b_6 = 2.893096381243585E5$
$b_5 = 6.908583833703266E4$
$b_4 = 6.274256335917373E3$
$b_3 = 1.814647140727353E2$
$b_2 = 1.407048742516088E0$

$$c_{12} = 3.076923000000000E0 \qquad c_{11} = 3.863046057270000E1$$
$$c_{10} = 1.554781665745842E3 \qquad c_9 = 1.742924336017660E4$$
$$c_8 = 9.040840730076884E4 \qquad c_7 = 2.124671765468546E5$$
$$c_6 = 1.947734149039538E5 \qquad c_5 = 5.973391309492905E4$$
$$c_4 = 5.995909210268758E3 \qquad c_3 = 1.792837888190744E2$$
$$c_2 = 1.407048742516088E0$$

$$d_{13} = 6.450000000000000E-3 \qquad d_{12} = 1.091615335000000E-1$$
$$d_{11} = 3.624185320350000E0 \qquad d_{10} = 5.091746847286805E1$$
$$d_9 = 3.547943683229924E2 \qquad d_8 = 1.336936456876723E3$$
$$d_7 = 2.683435732640813E3 \qquad d_6 = 2.676488788631499E3$$
$$d_5 = 1.219270697727660E3 \qquad d_4 = 2.070984356232960E2$$
$$d_3 = 1.095022353215910E1 \qquad d_2 = 1.177601945175335E-1$$

$$e_{11} = 1.984615335000000E-2 \qquad e_{10} = 2.412307632000000E-1$$
$$e_9 = 9.939789089966807E0 \qquad e_8 = 1.085217410408026E2$$
$$e_7 = 5.435258434733920E2 \qquad e_6 = 1.187537734225402E3$$
$$e_5 = 9.206973677068729E2 \qquad e_4 = 1.903702381877193E2$$
$$e_3 = 1.076769525553377E1 \qquad e_2 = 1.177601945175335E-1$$

References

[1] G. C. Ambrosini, T. Bozzoni, G. Cipollina, E. Colussi and R. Garroni, "Stability analysis and dynamic performance of a chemical system operated for the automatic fine control of a nuclear reactor," *Peaceful Uses of Atomic Energy Proceedings of the Third International Conference Geneva,* vol. 4, pp. 118-127, 31, Aug.-Sept. 1964.

[2] L. Eisenberg, "Stability of linear system with transport lag," *IEEE Trans. Automatic Contr.,* vol. AC-11, no. 2, pp. 247-254, April, 1966.

[3] C. L. Hu and K. W. Han, "Stability analysis of a nuclear reactor control system with multiple transport lags," *IEEE Trans. Nuclear Sci.,* vol. NS-20, no. 2, pp. 83-93, April 1973.

[4] D. D. Šiljak, "Analysis and synthesis of feedback control systems in the parameter plane," pt. I—Linear continuous systems, pt. II—Sampled-data systems, pt. III—Nonlinear systems," *IEEE Trans. Applications and Industry,* vol. 83, pp. 449-473, Nov. 1964.

[5] ——, "Generalization of parameter plane method," *IEEE Trans. Automatic Control,* vol. AC-11, no. 1, pp. 63-70, Jan. 1966.

[6] K. W. Han and G. J. Thaler, "Control system analysis and design using a parameter space method," *IEEE Trans. Automatic Contr.,* vol. AC-11, no. 3, pp. 560-563, July 1966.

[7] ——, "High order system analysis and design using the root locus method," *Journal of the Franklin Institute,* vol. 281, no. 2, pp. 99-113, Feb. 1966.

[8] K. W. Han, *Nonlinear Control Systems, Some Practical Methods.* Santa Clara, CA: Academic Culture, 1977.

[9] G. R. Keepin, T. F. Wimett, and R. K. Zeigler, "Delayed neutrons from fissionable isotopes of uranium, plutonium, and thorium," *Phys. Rev.,* vol. 107, pp. 1044-1049, 1957.